Molecular orientation, thermal behavior and density of electron and hole transport layers and the implication on device performance for OLEDs

Kenneth L. Kearns,[a] Hong-Yeop Na,[b] Robert D. Froese, [a] Sukrit Mukhopadhyay, [a] Hunter Woodward,[a] Dean Welsh,[a] Timothy De Vries,[a] David Devore,[a] Peter Trefonas,[c] Liang Hong[d]
[a]The Dow Chemical Company, Midland, MI USA 48674
[b]The Dow Seoul Technology Center, 1-5 Seoku-dong Hwaseong-si, Gyeonggi-do, South Korea
[c]Dow Electronic Materials, 455 Forest Street, Marlborough, MA USA 01752
[d]Dow Elastomers, Electrical and Telecommunications, 727 Norristown Road, Springhouse, PA 19477

ABSTRACT

Recent progress has shown that molecular orientation in vapor-deposited glasses can affect device performance. The deposition process can result in films where the molecular axis of the glass material is preferentially ordered to lie parallel to the plane of the substrate. Here, materials made within Dow's Electronic Materials business showed enhanced performance when the orientation of the molecules, as measured by variable angle spectroscopic ellipsometry, was oriented in a more parallel fashion as compared to other materials. For one material, the anisotropic packing was observed in the as-deposited glass and was isotropic for solution-cast and annealed films. In addition, the density of an as-deposited *N,N′*-bis(naphthalene-1-yl)-*N,N′*-bis(phenyl)-2,2′-dimethylbenzidine (NPD) film was 0.8% greater than what was realized from slowly cooling the supercooled liquid. This enhanced density indicated that vapor-deposited molecules were packing more closely in addition to being anisotropic. Finally, upon heating the NPD film into the supercooled liquid state, both the density and anisotropic packing of the as-deposited glass was lost.

Keywords: OLED, anisotropy, device performance, glass transition, ellipsometry, density, surface dynamics, film formation

1. INTRODUCTION

Organic light emitting diode (OLED) device performance has progressed substantially and electronic devices are currently using this display technology. Despite these advances further optimizing lifetime and efficiency is vital to see OLED display technology grow into other application spaces. Much of the focus in the field has been on changing the chemical structures or device stack architecture to manipulate device performance. A relatively recent tool for changing device performance is modifying the chemical structure to modify the way molecules pack in the glass film when deposited from the gas phase.

Physical vapor deposition is used extensively to prepare OLED devices and manipulating the deposition conditions and structure of the molecule can affect device performance via changes in glass packing. Some of the first reports using vapor deposition and substrate conditions to modify the packing of glass-forming molecules was on oligothiophenes.[1,2] Using optical methods, the deposited oligothiophenes preferentially oriented with the long axis of the molecule parallel to the substrate. In some cases, the nature of the substrate could be modified to alter the orientation to where the molecules would lie perpendicular to the substrate.[1] The substrate temperature has also been shown to affect the extent of anisotropy of the deposited layer.[3,4,5,6] The role vapor-deposition plays on the packing of small molecules and the effect packing has on device relevant properties has been studied in several materials. Charge transport materials were shown to have higher mobility in the direction perpendicular to the substrate when the linear or planar molecules were deposited such that they lied parallel to the plane of the substrate.[4,7,8, 9] Additionally, devices with lower turn-on voltages have been fabricated when the injection layer packed anisotropically.[10] Focus has also been paid to the orientation of the actively emitting molecule in the emissive layer where light outcoupling was enhanced if the molecule was oriented parallel to the substrate.[11, 12, 13, 14]

Organic Light Emitting Materials and Devices XVIII, edited by Franky So, Proc. of SPIE Vol. 9183, 91830F
 · doi: 10.1117/12.2062991

Here we will discuss the effect of anisotropy on device performance for several charge transport layers developed at The Dow Chemical Company for OLED applications. Both hole and electron transport materials were investigated. Correlations between device performance and material properties were made; material anisotropy correlated with device lifetime (i.e. a statistically significant correlation was observed). This was not the case between anisotropy and the other device performance metrics (power efficiency, current efficiency, turn-on voltage). Relative HOMO values could not explain differences in device performance for the hole transport layer (HTL) materials. In the case of the electron transport layer (ETL) materials, both the anisotropy and the relative LUMO values could explain device performance. For one of the HTL materials studied, solution cast films were also made. The packing in the spun-cast film was isotropic unlike the vapor-deposited glass.

Finally, changes to the films with thermal cycling will be discussed. The density of the as-deposited small molecule glass *N,N′*-bis(naphthalene-1-yl)-*N,N′*-bis(phenyl)-2,2′-dimethylbenzidine (NPD) was 0.8% denser than the glass prepared by slowly cooling the supercooled liquid. This behavior has been observed for small molecule, non-OLED glasses.[5, 6] NPD is shown as a case study for this behavior in OLED relevant materials. As NPD films were heated, a temperature was reached where the anisotropic, dense glass transformed into the supercooled liquid resulting in a material which had rarefied and lost the anisotropy realized during the deposition procedure. The anisotropy loss in NPD was consistent with observations made on HTL A; the anisotropy of as-deposited HTL A approached zero after annealing above T_g.

2. EXPERIMENTAL

2.1 Thin film preparation

Vapor deposition was carried out using an Åmod deposition chamber from Angstrom engineering. Undoped silicon wafers with a crystallographic orientation of <1 0 0> and a native oxide (Virginia Semiconductor Inc.) were mechanically affixed to the substrate holder using aluminum clips. The substrate holder was placed on a substrate stage which rotated at a rate of approximately 60 rpm. The pressure of the vacuum chamber prior to deposition was on the order of 10^{-7} Torr. A pneumatically controlled shutter was used to start and stop the deposition. A deposition rate of 2 Å/s was used for all films and the rate was maintained to within ± 10% throughout the duration of the deposition. The final thickness of the vapor-deposited film was nominally 50 nm. The absolute thickness was determined using variable angle spectroscopic ellipsometry.

Spun-cast films were also prepared for one of the materials as a comparison point to the evaporated material. A 2.0 wt% solution of the HTL material was made from anisole (Sigma-Aldrich, HPLC grade). The solution was filtered through a 400 μm Teflon ™ syringe filter and flooded onto the silicon wafer. The spinning rate of the spin-coater (Headway Research Inc. Model PWM32) was increased to 2000 rpm and held for 1 minute. The residual solvent was removed by placing the wafer into a vacuum oven overnight. The temperature of the wafer was held near the T_g of the material.

2.2 Full device preparation and performance characterization

To fabricate OLED devices, ITO coated glass was cleaned by sonication in acetone followed by sonication in isopropyl alcohol. Plasma treatment was then carried out. All organic materials were deposited thermally in a vacuum chamber operating near $1x10^{-7}$ Torr. The standard OLED device structure was composed of a hole injection, hole transport, emissive, electron transport and electron injection layers of a particular thickness. The thicknesses and device stack architecture was fixed in each device. Only the hole transport or electron transport layer was changed for relative comparisons. An 80 nm thick Al layer was used as the cathode. The deposition rate of the organic and Al layers was 1Å/s and 3Å/s, respectively.

The current density-voltage (J-V) and luminance-voltage (L-V) characteristics of OLEDs were measured using Keithley SMU 238 Source Measure Unit and Minolta CS-100A Color and Luminance Meter, respectively. The lifetime characteristics were measured by Polaronix® M6000S OLED Lifetime Test System.

2.3 Variable angle spectroscopic ellipsometry (VASE)

Variable angle spectroscopic ellipsometry (VASE) was carried out on an M-2000D ellipsometer from the J. A. Woollam Company. The wavelength range extended from 193 to 1000 nm via deuterium and quartz tungsten halogen lamps. Focusing optics were used during data collection. The incident angle for data collection was varied from 45 to 70 degrees as measured from surface normal of the substrate. Data from six different incident angles was taken in 5 degree increments.

For the thermal cycling experiment, a 2×2 cm square of silicon wafer with the vapor-deposited film was placed on an Instec thermal stage (model mK1000). The incident angle of the light beam was fixed at 70 degrees and the focusing optics were removed. An overhead camera was used to confirm the absence of macroscale crystallization during thermal treatment. The stage was heated from room temperature to temperatures above the glass transition temperature of the material (at least T_g+20). The heating and cooling rate was maintained at 2 $^{\circ}$C/min. Prior to the measurements, the thermal stage was calibrated at Instec. The temperature calibration was confirmed using octadecanoic acid, benzoic acid and 4-methoxy-benzoic acid melting point standards as well as the glass transition temperature of polystyrene. The 575 nm thick polystyrene film was cast onto a silicon wafer substrate from toluene, which was removed in a similar manner as the spun-cast HTL material.

2.4 Modeling of VASE data

Anisotropic general oscillator (GenOsc) models were used to characterize the raw psi and delta data collected at multiple angles by the ellipsometer using CompleteEase software (version 4.90) provided by J. A. Woollam Company. This model type was only used for the measurements made using multiple incident angles at ambient temperatures. Tauc-Lorentz and Gaussian oscillators were used to describe the absorption of the molecules. The amplitude, breadth, and energy of all oscillators were allowed to fluctuate during the modeling. A uniaxial anisotropic model was used where the z-axis optical properties, where the z-axis is orthogonal to the plane of the substrate, are allowed to be different than the optical properties in the x-y plane. The index described by the x-y plane and z-axis are referred to as the ordinary and extraordinary indices of refraction, respectively. Anisotropy, as measured by the difference in ordinary [n(o)] and extra-ordinary [n(e)] index of refractions, and thickness were reported.

Anisotropic Cauchy models were used for thermal cycling experiments on NPD. Thickness, A_{x-y}, B_{x-y}, A_z, and B_z were fit simultaneously over the entire temperature cycle. The Cauchy parameters A and B describe the dispersion of the index of refraction. For anisotropic Cauchy models, separate dispersion parameters were obtained to describe the index of refraction in the x-y plane and the z-axis. The wavelength range used for the Cauchy modeling was limited from 500 to 1000 nm where the extinction coefficient was zero. Thicknesses and differences in the ordinary and extraordinary indices of refraction were collected as a function of temperature.

2.5 Modeling of HOMO and LUMO levels

The ground-state (S_0) configurations of HTL and ETL molecules were computed using Density Functional Theory (DFT) at the B3LYP/6-31g level. The energies of highest occupied molecular orbital (HOMO) and lowest unoccupied molecular orbital (LUMO) are obtained from the S_0 configuration. The excited-state (S_1) energies and transition dipole moments are computed using time dependent density functional theory (TDDFT) in the ground-state configuration. All calculations are performed using G09 suit of programs.

3. RESULTS

Figure 1 shows the raw ellipsometric response as well as the modeling results from a 50 nm thick film of HTL A. The model fits the data well; the mean squared error (MSE) between the data and fit was 6.1 for the anisotropic general oscillator model fit. An isotropic general oscillator model resulted in an MSE of 27.2. The four-fold improvement in MSE was consistent with the additional model complexity being real; a 20% improvement in MSE with added model complexity is a rule of thumb to assess if the added complexity is justified. The need for an anisotropic model to fit the data well for HTL A indicated that the packing of the material was indeed anisotropic.

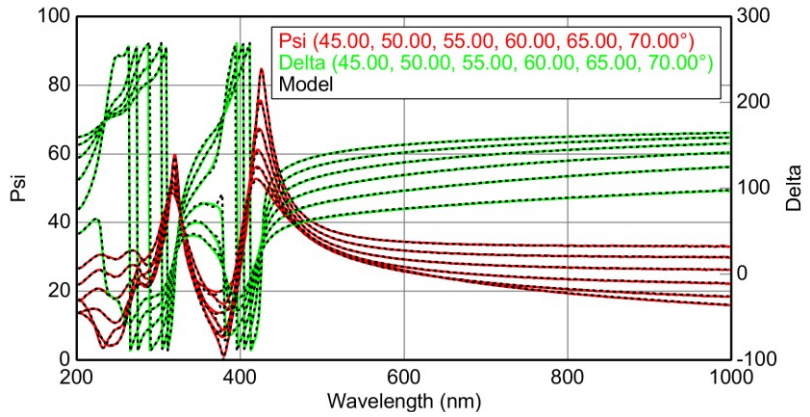

Figure 1: Variable angle spectroscopic ellipsometry data taken on a vapor-deposited 50 nm thick film of HTL A. The experimentally obtained psi (red) and delta (green) data are shown along with the anisotropic GenOsc modeling results (dashed, black line). The incident angles, relative to the surface normal, are given in the figure legend.

Once the need for an anisotropic model was established, the optical constants were investigated for the materials designed and tested at Dow. Figure 2 shows the differences in the index of refraction, n, and extinction coefficient, k, for two different HTL materials (panels A and B) and three different processing conditions for HTL A: vapor-deposited, annealed, and solution cast (panels A, C, and D, respectively). For each panel in Figure 2, the scale of the left y-axis, denoted n, is shown with the same scale for ease of comparison. For the two deposited materials, HTL A and HTL C, the ordinary, n(o), and extra-ordinary, n(e), indices of refraction were different over the visible wavelengths (400 – 1000 nm). Values for the ordinary index of refraction, which lies in the plane of the substrate, were greater than the orthogonal extra-ordinary index. This was consistent with molecules lying with the molecular axis more parallel to the plane of the substrate. The difference between n(o) and n(e) was larger for HTL A than HTL C indicating that the molecular axis of HTL A was lying more parallel to substrate than HTL C. This had implications for device performance and will be discussed below.

The ability of HTL A to lie parallel to the substrate was dependent on the processing method. This is shown graphically in panels A, C and D in Figure 2. While the vapor-deposited HTL A showed anisotropic packing, the annealed and solution-cast films showed essentially no anisotropic packing–n(o) and n(e) were nearly equivalent. The difference in packing can be rationalized by enhanced surface dynamics where the mobility of the surface is orders of magnitude faster at the top surface than in the bulk. Physical vapor deposition can take advantage of the enhanced dynamics. This mechanism is described in more detail below.

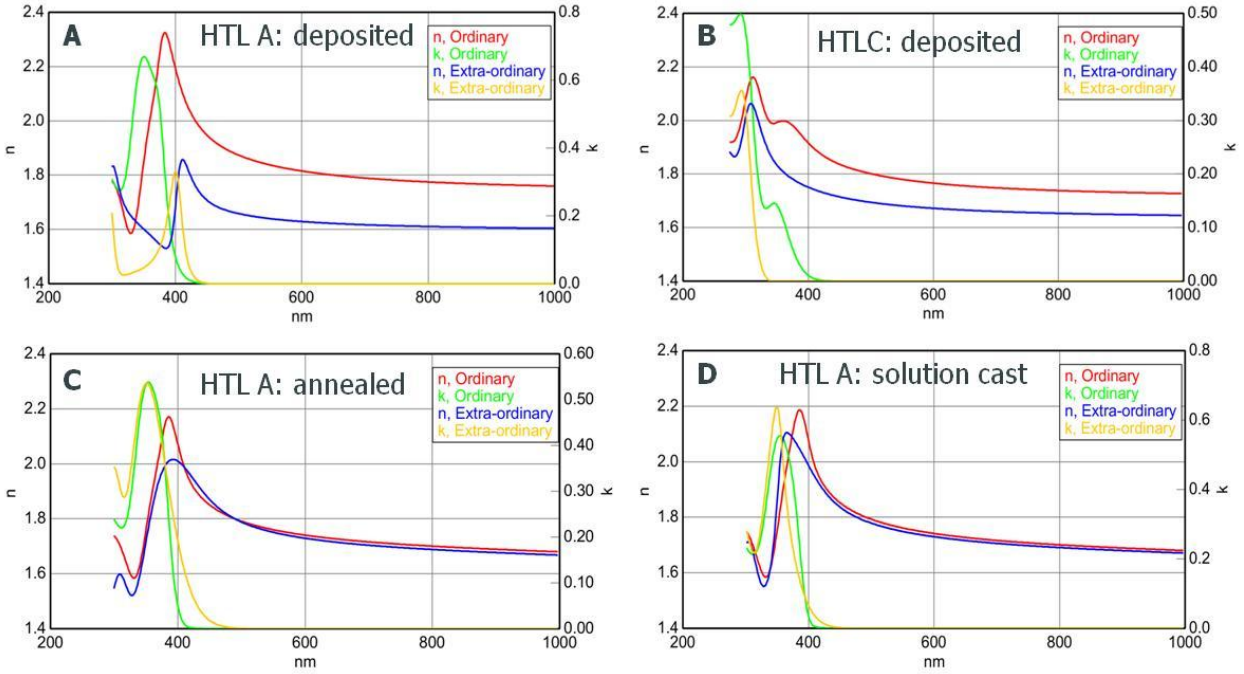

Figure 2: Index of refraction, n, and extinction coefficient data, k, obtained from model fits to VASE data for two different HTL materials. HTL A is also shown as a function of processing condition. The ordinary and extra-ordinary indices of refraction are shown as red and blue lines, respectively. Ordinary and extra-ordinary extinction coefficients are shown as the green and yellow lines, respectively.

Even though both HTL A and HTL C showed signs of anisotropic packing, the extent of the anisotropy was larger in HTL A. Better device performance was also observed in HTL A in comparison to HTL C. Figure 3 shows full device results for vapor-deposited devices of HTL A and HTL C. The more anisotropic HTL A outperformed HTL C in all three tests. Panel A shows the current density of the device with increasing voltage. HTL A turned on more than one volt lower than HTL C. The luminance efficiency was also greater for HTL A as shown in panel B. The device lifetime is an essential parameter for OLED manufacturers and panel C shows that HTL A clearly outperformed HTL C.

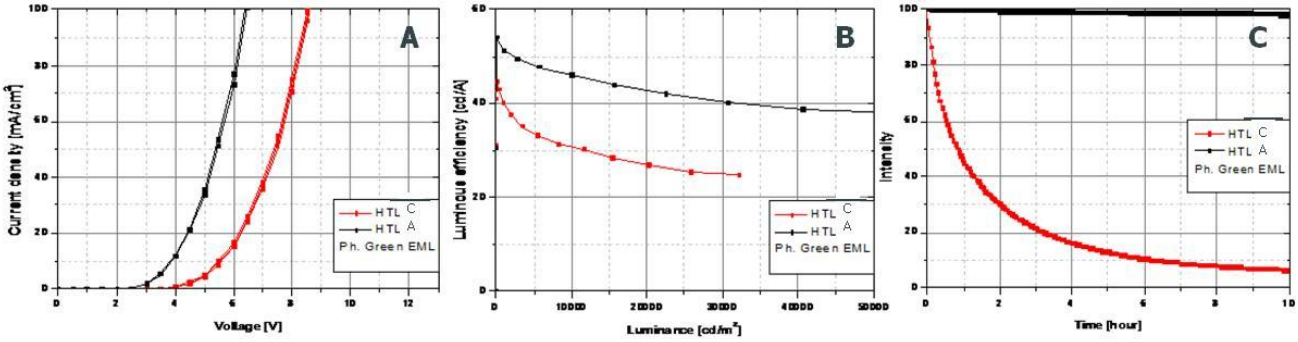

Figure 3: Characterization data from two devices where the HTL layer varied. Device data from HTL A is shown in black while HTL C is shown in red. Current density vs. voltage, luminance efficiency vs. luminance and device lifetime are shown in panels A, B, and C, respectively.

The correlation between anisotropy and device lifetime can be extended beyond these two materials. Several ETL and HTL materials are under development to improve the lifetime of an operating OLED along with the current-voltage and luminance efficiency characteristics. Figure 4 shows the correlation between device lifetime for full devices against the anisotropy (n(o) − n(e) at 632.8 nm) for both classes of materials. To compare the ETL materials, only the ETL material type was varied in the full device while keeping all of the materials and thicknesses in adjacent layers the same. The same protocol was used for the HTL materials. In both cases, there was a statistically significant correlation between

device lifetime and anisotropy. The correlation coefficient (R^2) was approximately 0.7 for the linear regression model used. The F-test from an analysis of variance (ANOVA) regression analysis also indicated that the linear regression model was statistically significant due to the fact that the Prob>F values were less than 0.05. Lower values of Prob>F indicate more statistically significant regression models with 0.05 being an upper bound for what signifies as a statistically significant result.[15]

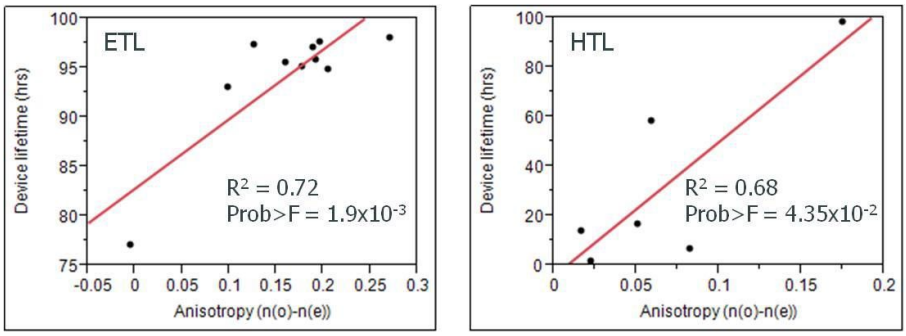

Figure 4: Correlation of device lifetime with anisotropy (n(o)−n(e) measured at 632.8 nm) for the HTL and ETL materials studied in this proceeding. The correlation coefficient (R^2) and the results of the F-test for an analysis of variance (ANOVA) are given for each material type.

Device lifetime is not the only important device property nor is anisotropy the only material property that is important for device performance. Table 1 and Table 2 list the statistical analysis results from linear regression analysis between various device performance metrics and either the HOMO, LUMO or n(o)−n(e) values. The electronic characteristics of the material are important for getting charge across the layers of the device. The HOMO and LUMO values dictate the ease of hole and electron injection into the HTL and ETL, respectively. For the HTL materials, the correlation between the device lifetime and n(o)-n(e) was higher than for any other combination of device performance listed; the correlation coefficient (R^2) and F-test from the ANOVA (Prob>F) were the highest and lowest, respectively. This statistical analysis points towards the n(o)−n(e) being an important material characteristic for optimum device performance. Of course, HOMO, LUMO, and n(o)−n(e) values are a narrow set of characterization parameters and other material properties will play a role in performance. Nonetheless, the strength of the correlation relative between device performance and n(o)−n(e) is striking.

The correlation between device performance and n(o)−n(e) for ETL materials is more complicated. Once again we observed a comparatively strong statistical correlation between anisotropy and device lifetime; however, a strong correlation was also observed between device lifetime and LUMO. An experiment where the LUMO of the materials studied is similar but the n(o)−n(e) varies, or vice versa, is needed to assess the relative performance of each parameter. For the class of ETL compounds studied, materials with these characteristics were not targeted but would be important for future studies.

Table 1: Statistical results from linear regression fits of device parameters vs. HTL material property of interest–n(o)−n(e) or calculated HOMO level. The correlation coefficient (R^2) and F-test results from ANOVA are tabulated.

HTL device statistics			
vs.		**R^2**	**Prob>F**
device lifetime	n(o)-n(e)	0.68	0.04
power efficiency	n(o)-n(e)	0.09	0.56
voltage at 1000 nit	n(o)-n(e)	0.09	0.56
current efficiency	n(o)-n(e)	0.00	0.90
device lifetime	HOMO	0.47	0.13
power efficiency	HOMO	0.00	0.93
voltage at 1000 nit	HOMO	0.01	0.87
current efficiency	HOMO	0.12	0.49

Table 2: Statistical results from linear regression fits of device parameters vs. ETL material property of interest–n(o)−n(e) or calculated LUMO level. The correlation coefficient (R^2) and F-test results from ANOVA are tabulated.

ETL device statistics			
vs.		**R^2**	**Prob>F**
device lifetime	n(o)-n(e)	0.72	0.00
power efficiency	n(o)-n(e)	0.03	0.62
voltage at 1000 nit	n(o)-n(e)	0.08	0.43
current efficiency	n(o)-n(e)	0.15	0.28
device lifetime	LUMO	0.77	0.00
power efficiency	LUMO	0.21	0.18
voltage at 1000 nit	LUMO	0.00	0.89
current efficiency	LUMO	0.35	0.07

The density and thermal behavior of vapor-deposited materials were also studied in a common OLED material. Temperature dependent spectroscopic ellipsometry data on NPD is shown in Figure 5. The first heating of the sample was unique from the second in several ways. First, as the vapor-deposited glass was initially heated (black line), the thickness of the glass changed according to the coefficient of thermal expansion (CTE) of the material; the slope of the black line from 300 to 360 °C in Figure 5 is the CTE of the glass. Upon heating this material to temperatures between 380 and 385 °C, the material quickly expanded until it finally became a supercooled liquid at temperatures above 385 °C. The temperature where this transformation began is defined by the intersection of the dashed, gray lines in Figure 5 and is denoted as T_{onset}. This temperature has been defined in a similar manner by others in the literature.[5, 6] The material was in the supercooled liquid state at temperatures above 385 °C. The CTE of the supercooled liquid was greater than the glass CTE as indicated by the greater slope. Second, the density of the as-deposited glass (black line) was greater than the glass made after cooling the glass from the supercooled liquid state. This density difference, as measured by the thickness difference, was 0.8 %.

Once the sample was transformed into a supercooled liquid, the NPD sample behaved as expected for an ordinary amorphous system. As the NPD was cooled from the upper temperature limit, the supercooled liquid underwent a glass transition. This was signified by the change in CTE between the supercooled liquid and glass. The temperature of this transition was determined by the intersection between the dotted and dash-dotted gray lines in Figure 5. The temperature of the transition is denoted as $T_{g, OG}$ in the figure–the glass transition (T_g) of the ordinary glass (OG) formed from cooling the supercooled liquid. The second heat of the glass nearly retraced the cooling curve as expected for an ordinary glass. The enhanced density realized by the vapor deposition was not observed during the second heating scan.

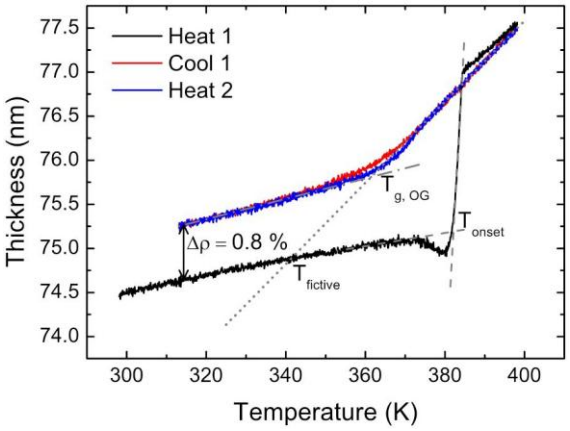

Figure 5: Thickness vs. temperature data for a nominally 75 nm thick NPD film vapor-deposited onto a silicon wafer with native oxide. A heat-cool-heat thermal profile performed at a rate of ±2 °C/min was used and is shown as the black, red and blue lines, respectively.

Changes to the anisotropy, as measured by the difference between n(o) and n(e), were also studied on the same NPD film during thermal cycling. Figure 6 shows results from the same heat-cool-heat experiment on the same sample used to obtain the data shown in Figure 5. The as-deposited glass sample showed evidence for anisotropic packing; initial values

of n(o)−n(e) were near 0.06. As the sample was heated, this anisotropy value decreased. An abrupt loss of anisotropy was observed near 380 °C. This was the same temperature regime as the thickness change in Figure 5. After the abrupt change in anisotropy, the n(o)−n(e) values were near zero. As was observed for the density of NPD, the vapor-deposited glass loses anisotropy once it is heated to sufficiently high temperatures and never regains the anisotropy upon further thermal cycling.

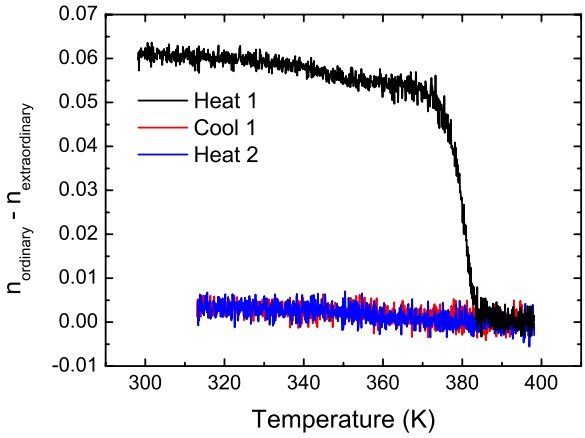

Figure 6: Difference between the ordinary and extraordinary indices of refraction as a function of temperature for a nominally 75 nm thick NPD film. A heat-cool-heat thermal profile performed at a rate of ±2 °C/min was used, and the results are shown as the black, red and blue lines, respectively.

4. DISCUSSION

The discussion below will focus on three main aspects of the data. First, the effect of anisotropy on device performance will be addressed. Second, the effect of processing on the material anisotropy will be presented. An enhanced surface dynamics mechanism will be discussed which explains the observed anisotropy differences between the vapor-deposited, spun-cast and annealed films. Finally, the observed density for NPD and the effect thermal annealing has on density, as well as anisotropy, will be discussed.

4.1 Anisotropy and device performance

Several materials properties are important to fabricate a highly functioning OLED: the energy levels of the HOMO and LUMO need to be well matched between adjacent layers, mobility of charges through the layer must be optimized, the layers must be robust both thermally and chemically, the device needs to efficiently convert electrical charge into usable light, etc. Few materials, and combinations of materials, can simultaneously fulfill all of these requirements.

Molecular level anisotropy can aid device performance in many ways. If molecules are packed within a layer such that the adjacent molecules within the layer interact strongly via high π-π orbital overlap, mobility through the layer can be enhanced.[7, 8] This overlap may also result in fewer traps within the layer allowing for more efficient device performance. The anisotropic packing can lower charge injection barriers resulting in lower operating voltages and ultimately less power consumption during use.[10] As molecules pack more anisotropically, the HOMO and LUMO levels near the interface can change and allow for easier transport across discrete layers.[16] The outcoupling of light can also become more efficient where plasmonic and total internal reflection losses are minimized.[11]

Despite the importance of anisotropic packing within a vapor-deposited glass layer, this material property is not a panacea for all of the requirements listed at the beginning of this section. As HOMO and LUMO levels, mobility, and robustness concerns are optimized, anisotropy becomes an important factor for moving the overall device performance even higher and potentially broadening application space to larger scale devices.

The observation of the correlations between the measured anisotropy in the layer that was exchanged in the device stack and lifetime is striking. Each of the performance metrics presented in Table 1 and Table 2 could be affected by

anisotropy in some way. Why device lifetime correlates well for both HTL and ETL is not clear. Device lifetime is a property which is dependent on many factors. The properties of the charge transport layers may be optimized such that several anisotropy dependent properties are optimized resulting in a cumulative effect that improves lifetime. More work needs to be done to understand these relationships.

4.2 Role of deposition process on anisotropy

Understanding the role of processing conditions on small molecule glass-formers is a relatively young field; nonetheless, some of the first measurements were obtained from vapor-deposited electronic materials. Vapor deposition of oligothiophene molecules of various length were shown to exhibit preferential packing where the long axis of the molecule was lying down on the substrate.[1] The opposite case could also be true where the molecule is standing up depending on the nature of the substrate. More recently, several researchers have explored the role of deposition methods and conditions on the level of anisotropy and how this affects application relevant properties.[3, 4, 7, 8, 9, 10, 11, 12, 13, 14]

OLED layers can be deposited by either a vapor based process or a liquid based process. Both result in thin films, but the resulting material properties can be quite different. Recently, vapor deposition and solution casting of the same molecule resulted in anisotropic packing and enhanced device performance when vapor-deposited, but isotropic packing was observed for solution casting resulting in poorer device performance.[17] Anisotropic packing can be obtained in both solution casting as well as vapor deposition; however, to obtain the anisotropic packing for both processing methods, the molecular design needs to be altered to take advantage of the driving forces associated with each mechanism.

The strength of the intermolecular interactions between molecules is important for producing anisotropic materials in solution cast films. At early times in the film formation process, the layer is a mixture of the molecule of interest and the solvent used to make the solution. This initial film will be isotropic. As the film dries, the distance between molecules is shortened and the strength of the intermolecular interactions takes over. This was the case for poly (amide-imide) films cast from dimethylacetamide.[18] The initially cast film showed little difference between the ordinary and extraordinary indices of refraction. As the several micron thick film dried over 16 hours, a strongly birefringent film formed where the plane of the molecule preferentially oriented itself parallel to the substrate. The lack of anisotropy in the present study for a solution cast film may have been due to either a lack of sufficient intermolecular interactions or the timescale of drying in spin coating was much too fast to take advantage of these interactions. External forces on the molecules themselves, either during or after casting, can be used to orient molecules in the film, but this was not explored here.

For vapor-deposited films, the interplay between the dynamics at the film/vacuum interface as well as the thermodynamics of the depositing material relative to the substrate temperature during deposition are important. During vapor deposition, each molecule in the film experiences some time at the film/vacuum interface. The dynamics at this interface are several orders of magnitude faster than the bulk dynamics at the given temperature.[19] The enhanced surface dynamics gives molecules the ability to rearrange and sample many configurations resulting in an optimized glass packing geometry. If the temperature of the substrate is significantly below the bulk T_g for the system, the molecules at the interface can move quickly as compared to the bulk and realize a thermodynamic driving force that pushes the system towards the metastable, equilibrium supercooled liquid (assuming no crystal formation). If the substrate temperature is near the bulk T_g, the thermodynamic driving force is negligible despite the enhanced surface dynamics.[20] Conversely, at temperatures far below T_g, the driving force to optimize the glass packing is strong, but the dynamics are too slow to effectively sample configuration space.

4.3 Material density and anisotropy with thermal treatment

The density of vapor-deposited NPD glass was shown to be 0.8% greater than the glass prepared by controlled cooling from the supercooled liquid. The enhanced density of the vapor-deposited material is likely to be advantageous for charge transport through an electron or hole transport layer. The density of the glass layer depends on the material itself and the free volume between molecules. If the density of the system is greater but the molecule has not changed, the free volume between adjacent molecules must decrease due to the fixed size of the molecule. Ultimately, the distance between the molecules is smaller. As the intermolecular distance decreases, the molecular orbitals on adjacent molecules can interact to a greater extent and facilitate charge hopping from one molecule to the next. This is particularly true if the packing is anisotropic in nature. The ability to pack more densely can be attributed to the enhanced dynamics resulting in more optimized packing.

The ability to pack vapor-deposited NPD more densely is not likely to be unique to this molecule. Vapor-deposited 1,3,5-trisnaphthylbenzene, TNB,[5] indomethacin,[6] toluene, ethylbenzene, propylbenzene and isopropylbenzene[21, 22] have all shown the ability to pack more densely than the glass prepared by controlled cooling from the supercooled liquid state. If the deposition conditions were controlled appropriately, density could be 1.2 to 1.3 percent greater for indomethacin and TNB, respectively. The density in each case was optimized by slow deposition rates near 1 to 2 Å/s and substrate temperatures 85% below the bulk glass transition temperature on the Kelvin scale. When the substrate temperature was closer to the bulk T_g during deposition, the vapor-deposited glass became less dense. For the case of the glasses made from substituted benzenes, the density of the as-deposited glass was different than the glass prepared by controlled cooling; however, the experimental technique used to collect this data was not sensitive to the birefringence of the film and thus complicated the density measurement.

As with density, anisotropy of the vapor-deposited NPD films was also susceptible to the thermal treatment of the layer. The differences in anisotropy between panels A and C of Figure 1 for HTL A were consistent with the results shown in Figure 6 for NPD; the as-deposited glass packed anisotropically while the film became isotropic after heating to sufficiently high temperatures. The vapor-deposition process once again allowed for the enhanced dynamics of the surface to sample configuration space and pack in a way that was more anisotropic. The dynamics in the bulk of the system could not accomplish the anisotropic packing as observed by the lack of any significant change in anisotropy or density on cooling from the supercooled liquid.

Finally, the thermal robustness of vapor-deposited NPD glass was greater than the robustness observed for the glass prepared by controlled cooling of the supercooled liquid. The transition temperature of the vapor-deposited glass into a supercooled liquid was higher than the glass transition temperature observed for the glass prepared by controlled cooling from the supercooled liquid. This difference in transition temperature has implications for the T_g requirements of a material. By vapor-depositing the glass, the transition temperature can be increased by ~20 K in NPD. Similar temperature shifts have been observed in other non-OLED, vapor-deposited glass systems.[5, 6] The bulk glass transition temperature is still important for thermal requirements, but it should be pointed out that the bulk glass transition temperature measured on a glass cooled from the supercooled liquid state may not be a true representation of the transition temperature of the vapor-deposited material.

5. CONCLUSIONS

Anisotropy plays an important role in device performance of fully functioning devices. Anisotropy was quantified using variable angle spectroscopic ellipsometry in several HTL and ETL materials that were synthesized at The Dow Chemical Company. Anisotropy was determined as the difference between the ordinary and extraordinary index of refraction at 623.8 nm. It was shown here that there was a strong correlation between the measured anisotropy of an ETL or HTL molecule and device lifetime. A correlation was not observed between other device performance metrics and the anisotropy. The HOMO energy levels of the HTL did not correlate well with lifetime, but the LUMO energy levels of the ETL did. Specific experiments are needed to determine which parameter is responsible for the correlation in ETLs.

Film processing was shown to affect the observed anisotropy; solution cast films were isotropic unlike the vapor-deposited film. The difference in observed anisotropy was attributed to differences in how the layer was formed and if the formation process was able to take advantage of the enhanced dynamics anticipated to be at the top surface of the film. The entire film could take advantage of these dynamics during vapor deposition, whereas solution casting must rely on strong intermolecular interactions.

For vapor-deposited NPD samples, which were originally anisotropic and more dense than the glass cooled from the supercooled liquid, thermal treatment removed the anisotropy and density. Thermal treatment was also shown to affect the level of anisotropy observed in HTL A; the material packing became isotropic after being heated to above its glass transition temperature. Finally, the temperature where the glass transformed into a supercooled liquid and lost the anisotropic packing and higher density was ~20 K greater than the glass transition temperature of the NPD glass made by controlled cooling of the supercooled liquid.

ACKNOWLEDGEMENTS

The authors would like to acknowledge the synthesis and purification efforts of the team: Kaitlyn Gray, Kyoung-Moo Koh, Nolan McDougal, Mark Ondari, Liam Spencer, Tony Tang, Jean Yan and Tomas Paine.

REFERENCES

[1] Oelkrug, D., Egelhaaf, H. J., & Haiber, J., "Electronic spectra of self-organized oligothiophene films with 'standing' and 'lying' molecular units," Thin Solid Films 284, 267-270 (1996).

[2] Egelhaaf, H. J., Gierschner, J., Haiber, J., & Oelkrug, D., "Optical constants of highly oriented oligothiophene films and nanoparticles," Optical Materials 12(2), 395-401 (1999).

[3] Yokoyama, D., Adachi, C., "In situ real-time spectroscopic ellipsometry measurement for the investigation of molecular orientation in organic amorphous multilayer structures," J. Appl. Phys. 107(12), 123512 (2010).

[4] Yokoyama, D., "Molecular orientation in small-molecule organic light-emitting diodes," J. Mat. Chem. 21(48), 19187-19202 (2011).

[5] Dalal, S. S., Sepúlveda, A., Pribil, G. K., Fakhraai, Z., & Ediger, M. D., "Density and birefringence of a highly stable α,α,β-trisnaphthylbenzene glass," J. Chem. Phys. 136(20), 204501 (2012).

[6] Dalal, S. S., Ediger, M. D., "Molecular orientation in stable glasses of indomethacin," J. Phys. Chem. Lett. 3(10), 1229-1233 (2012).

[7] Yokoyama, D., Sasabe, H., Furukawa, Y., Adachi, C., & Kido, J., "Molecular Stacking Induced by Intermolecular C–H⋯ N Hydrogen Bonds Leading to High Carrier Mobility in Vacuum-Deposited Organic Films," Adv. Func. Mater. 21(8), 1375-1382 (2011).

[8] Yokoyama, D., Setoguchi, Y., Sakaguchi, A., Suzuki, M., & Adachi, C., "Orientation Control of Linear-Shaped Molecules in Vacuum-Deposited Organic Amorphous Films and Its Effect on Carrier Mobilities," Adv. Func. Mater. 20(3), 386-391 (2010).

[9] Yokoyama, D., Sakaguchi, A., Suzuki, M., & Adachi, C. "Enhancement of electron transport by horizontal molecular orientation of oxadiazole planar molecules in organic amorphous films," Appl. Phys. Lett. 95(24), 243303 (2009).

[10] Kim, J. Y., Yokoyama, D., & Adachi, C. "Horizontal Orientation of Disk-like Hole Transport Molecules and Their Application for Organic Light-Emitting Diodes Requiring a Lower Driving Voltage," J. Phys. Chem. C 116(15), 8699-8706 (2012).

[11] Brütting, W., Frischeisen, J., Schmidt, T. D., Scholz, B. J., & Mayr, C., "Device efficiency of organic light-emitting diodes: Progress by improved light outcoupling," Phys. Status Solidi A 210(1), 44-65 (2013).

[12] Nowy, S., Frischeisen, J., & Brütting, W., "Simulation based optimization of light-outcoupling in organic light-emitting diodes," SPIE Photonic Devices and Applications (pp. 74151C-74151C), (2009, August).

[13] Komino, T., Tanaka, H., & Adachi, C., "Selectively Controlled Orientational Order in Linear-Shaped Thermally Activated Delayed Fluorescent Dopants," Chem. Mater. 26(12), 3665-3671 (2014).

[14] Frischeisen, J., Yokoyama, D., Adachi, C., & Brütting, W., "Determination of molecular dipole orientation in doped fluorescent organic thin films by photoluminescence measurements," Appl. Phys. Lett. 96(7), 073302 (2010).

[15] Kanji, G. P., [100 Statistical Tests], SAGE Publications Ltd, London, (2006).

[16] Chen, W., Huang, H., Chen, S., Huang, Y. L., Gao, X. Y., & Wee, A. T. S. Molecular orientation-dependent ionization potential of organic thin films. Chem. Mater. 20(22), 7017-7021 (2008).

[17] Xing, X., Zhong, L., Zhang, L., Chen, Z., Qu, B., Chen, E., ... & Gong, Q., "Essential Differences of Organic Films at the Molecular Level via Vacuum Deposition and Solution Processes for Organic Light-Emitting Diodes," J. Phys. Chem. C 117(48), 25405-25408 (2013).

[18] Yucel, O., Unsal, E., & Cakmak, M., "Temporal Evolution of Optical Gradients during Drying in Cast Polymer Solutions," Macromolecules 46(17), 7112-7117 (2013).

[19] Zhu, L., Brian, C. W., Swallen, S. F., Straus, P. T., Ediger, M. D., & Yu, L., "Surface self-diffusion of an organic glass," Phys. Rev. Lett. 106(25), 256103 (2011).

[20] Kearns, K. L., Swallen, S. F., Ediger, M. D., Wu, T., Yu, L. "Influence of substrate temperature on the stability of glasses prepared by vapor deposition," J. Chem. Phys. 127(15), 154702 (2007).

[21] Ishii, K., Nakayama, H., Moriyama, R., & Yokoyama, Y., "Behavior of Glass and Supercooled Liquid Alkylbenzenes Vapor-Deposited on Cold Substrates: Toward the Understanding of the Curious Light Scattering Observed in Some Supercooled Liquid States," Bull. Chem. Soc. Jpn 82(10), 1240-1247 (2009).

[22] Ishii, K., Nakayama, H., & Moriyama, R., "Nonequilibrium and Relaxation in Deeply Supercooled Liquid of Isopropylbenzene Obtained through Glass Transition from Vapor-Deposited Glass," J. Phys. Chem. B, 116(3), 935-942 (2012).